



## Insulating-layer formation of metallic LaNiO<sub>3</sub> on Nb-doped SrTiO<sub>3</sub> substrate

Hyang Keun Yoo, Young Jun Chang, Luca Moreschini, Hyeong-Do Kim, Chang Hee Sohn, Soobin Sinn, Ji Seop Oh, Cheng-Tai Kuo, Aaron Bostwick, Eli Rotenberg, and Tae Won Noh

Citation: [Applied Physics Letters](#) **106**, 121601 (2015); doi: 10.1063/1.4916225

View online: <http://dx.doi.org/10.1063/1.4916225>

View Table of Contents: <http://scitation.aip.org/content/aip/journal/apl/106/12?ver=pdfcov>

Published by the [AIP Publishing](#)

---

### Articles you may be interested in

[Investigation of dislocations in Nb-doped SrTiO<sub>3</sub> by electron-beam-induced current and transmission electron microscopy](#)

*Appl. Phys. Lett.* **106**, 102109 (2015); 10.1063/1.4915298

[Fermi level shift in La<sub>2-x</sub>Sr<sub>x</sub>CuO<sub>4</sub> probed by heteroepitaxial junctions with Nb-doped SrTiO<sub>3</sub>](#)

*Appl. Phys. Lett.* **102**, 111606 (2013); 10.1063/1.4798252

[Electric field penetration in Au / Nb : SrTiO<sub>3</sub> Schottky junctions probed by bias-dependent internal photoemission](#)

*Appl. Phys. Lett.* **98**, 192103 (2011); 10.1063/1.3589375

[Orientation dependence of the Schottky barrier height for La<sub>0.6</sub>Sr<sub>0.4</sub>MnO<sub>3</sub> / SrTiO<sub>3</sub> heterojunctions](#)

*Appl. Phys. Lett.* **94**, 242106 (2009); 10.1063/1.3154523

[Band diagrams of spin tunneling junctions La<sub>0.6</sub>Sr<sub>0.4</sub>MnO<sub>3</sub>/Nb : SrTiO<sub>3</sub> and SrRuO<sub>3</sub>/Nb : SrTiO<sub>3</sub> determined by in situ photoemission spectroscopy](#)

*Appl. Phys. Lett.* **90**, 132123 (2007); 10.1063/1.2717517

---

The advertisement features a photograph of the Model PS-100 cryogenic probe station, a complex piece of scientific equipment with various lenses, sensors, and mechanical components. The background is a gradient of blue. On the left, the text 'Model PS-100' is in a large, bold, white font, with 'Tabletop Cryogenic Probe Station' below it in a smaller white font. On the right, the 'Lake Shore CRYOTRONICS' logo is displayed, with 'Lake Shore' in a large, white, serif font and 'CRYOTRONICS' in a smaller, white, sans-serif font below it. Below the logo, the tagline 'An affordable solution for a wide range of research' is written in a white, italicized serif font.

## Insulating-layer formation of metallic $\text{LaNiO}_3$ on Nb-doped $\text{SrTiO}_3$ substrate

Hyang Keun Yoo,<sup>1,2</sup> Young Jun Chang,<sup>3,4</sup> Luca Moreschini,<sup>4</sup> Hyeong-Do Kim,<sup>1,2,a)</sup>  
 Chang Hee Sohn,<sup>1,2</sup> Soobin Sinn,<sup>1,2</sup> Ji Seop Oh,<sup>1,2</sup> Cheng-Tai Kuo,<sup>1,2</sup> Aaron Bostwick,<sup>4</sup>  
 Eli Rotenberg,<sup>4</sup> and Tae Won Noh<sup>1,2</sup>

<sup>1</sup>Center for Correlated Electron Systems, Institute for Basic Science (IBS), Seoul 151-747, South Korea

<sup>2</sup>Department of Physics and Astronomy, Seoul National University, Seoul 151-747, South Korea

<sup>3</sup>Department of Physics, University of Seoul, Seoul 130-743, South Korea

<sup>4</sup>Advanced Light Source (ALS), E. O. Lawrence Berkeley National Laboratory, Berkeley, California 94720, USA

(Received 1 December 2014; accepted 14 March 2015; published online 23 March 2015)

We investigated the electronic structures of strongly correlated metallic  $\text{LaNiO}_3$  (LNO) and semiconducting Nb-doped  $\text{SrTiO}_3$  (Nb:STO) heterostructures by varying the LNO film thickness using *in situ* photoemission spectroscopy. We found that, contrary to other interfaces with  $\text{SrTiO}_3$  and  $\text{LaAlO}_3$ , insulating LNO layers are formed between metallic LNO layers and Nb:STO. Such behavior seems to be related with an electron transfer from Nb:STO to LNO due to Schottky-barrier formation at the interface. © 2015 AIP Publishing LLC.

[<http://dx.doi.org/10.1063/1.4916225>]

Semiconductor heterostructures play key roles in modern electronic devices.<sup>1</sup> In particular, Schottky barrier (SB) formation at a metal-semiconductor (MS) interface induces a rectifying *I-V* characteristic, so it has been utilized for various devices including diode applications.<sup>2</sup> However, conventional MS technology has almost reached its limit, prompting extensive research in an effort to overcome performance limitations.<sup>3</sup> A transition-metal-oxide (TMO) heterostructure is a potential solution because of its unique physical properties that provide enhanced functionality in electronic or spintronic devices.<sup>4–7</sup> For example, a SB at the interface between a conventional metal and a correlated TMO semiconductor has been used for memristive devices.<sup>6</sup> Additionally, heterostructures consisting of TMOs have recently been utilized for spintronic devices.<sup>7</sup>

$\text{SrTiO}_3$  (STO) is one of the most important and widely used materials for functional TMO electronics. Bulk STO is an uncorrelated nonmagnetic wide-bandgap semiconductor.<sup>8</sup> However, STO-based heterostructures exhibit many intriguing properties including memristive behavior,<sup>9</sup> two-dimensional (2D) electron gas,<sup>10</sup> magnetism,<sup>11</sup> and 2D superconductivity.<sup>12</sup> Similarly, bulk  $\text{LaNiO}_3$  (LNO) is a paramagnetic metal,<sup>13</sup> but numerous interesting phenomena, such as a charge/spin ordering<sup>14–16</sup> and potential high- $T_c$  superconductivity,<sup>17,18</sup> have been investigated in heterostructures. Thus, a heterostructure, composed of strongly correlated metallic LNO and semiconducting STO, can provide another interesting phenomena.

In this work, using *in situ* photoemission spectroscopy, we investigated the electronic structures of LNO and Nb-doped STO (Nb:STO) heterostructures by varying the LNO film thickness. We found that insulating LNO layers with a finite band gap are formed between metallic LNO and semiconducting Nb:STO, contrary to other LNO/STO and LNO/ $\text{LaAlO}_3$ (LAO)/Nb:STO heterostructures. Though the mechanism of the insulating-layer formation is not clear at present, the possible origin would be the SB formation at the

interface by an electron-transfer from Nb:STO to LNO. This result demonstrates that strongly correlated TMOs can show anomalous behavior different from that of the conventional MS heterostructure.

Ultrathin LNO films were grown on semiconducting Nb-0.5-wt. %-doped STO(001) substrates by pulsed laser deposition (PLD). Before PLD, atomically flat Nb:STO substrates were prepared by using buffered-hydrofluoric acid etching and heating processes. Then, we varied LNO film thickness from 10 to 2 unit cells (UC). We used a KrF excimer laser ( $\lambda = 248$  nm) with a repetition rate of 2 Hz to ablate sintered stoichiometric targets. The laser energy density was 1.0–1.5 J/cm<sup>2</sup> at the target position. Note that, to control for quality variation among films, we deposited all the films on the same substrate at once by choosing the deposited area selectively using a mechanical shutter.<sup>19</sup>

We monitored film quality during the growth using reflection high energy electron diffraction (RHEED). The RHEED patterns show that the LNO films have the same  $1 \times 1$  surface structure with that of Nb:STO(001). This result indicates that the surface reconstruction in the LNO films is negligible up to 10 UC. After deposition, films were transferred *in vacuo* to the analysis chamber with a base pressure of  $5 \times 10^{-11}$  Torr. The *in situ* photoemission spectroscopy measurements were performed at an end-station equipped with PLD at the Beamline 7.0.1 of the Advanced Light Source. The measurement temperature was kept at 90 K, and the total energy resolution is about 30 meV at  $h\nu = 150$  eV.

Figure 1 shows the angle-integrated valence-band spectra of LNO/Nb:STO heterostructures measured at  $h\nu = 200$  eV, varying the LNO film thickness from 10 to 2 UC. In the 10-UC LNO film, the two sharp peaks at around  $-0.8$  eV and near the Fermi level ( $E_F$ ) correspond to the  $t_{2g}$  and the  $e_g$  bands, respectively.<sup>20</sup> The broad O  $2p$  bands, including non-bonding and bonding states, are located at around 2–7 eV.<sup>20</sup> As the film thickness decreases, the  $t_{2g}$  bands gradually move away from  $E_F$  and the quasiparticle peak from the  $e_g$  bands is strongly suppressed. Below 3 UC,

<sup>a)</sup>Electronic mail: hdkim6612@snu.ac.kr

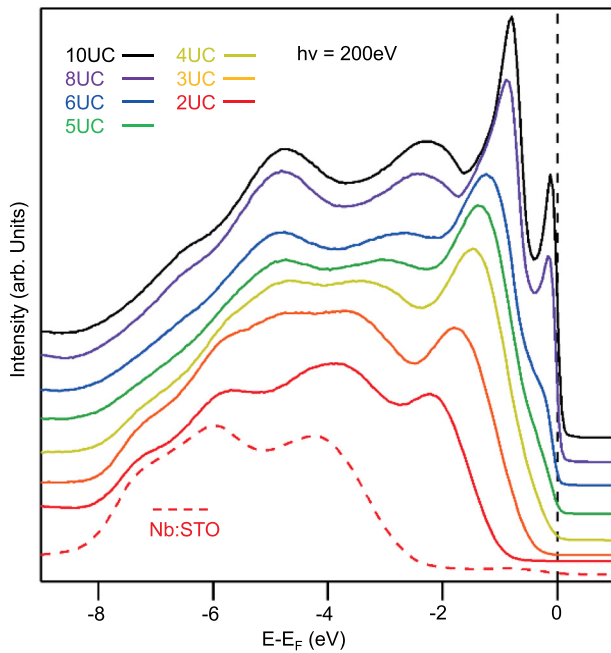


FIG. 1. Valence-band spectra of LNO/Nb:STO heterostructures with the film thickness from 10 to 2 UC obtained at  $h\nu = 200$  eV. For comparison, the valence-band spectra of Nb:STO are depicted by red dashed line.

the quasiparticle peak is completely removed, a finite insulating gap being opened. This result suggests that an unexpected insulating phase appears at the interface between correlated metal LNO and highly conducting semiconductor Nb:STO.

To more deeply understand the insulating layer formation in LNO/Nb:STO heterostructures, we carried out angle-resolved photoemission spectroscopy (ARPES), which are presented in Figs. 2(a)–2(c) for 10-, 6-, and 2 UC, respectively. The ARPES spectra of the 10-UC LNO film along the  $\Gamma XM$  and the  $ZRA$  lines consist of the nearly flat  $t_{2g}$  bands at  $-0.8$  eV and the dispersive  $e_g$  bands near  $E_F$ . This electronic structure is consistent with theoretical calculation of bulk LNO under tensile strain.<sup>21</sup>

As the film thickness decreases from 10 to 6 UC, the electronic-structure change is nearly the same with that of LNO films grown on an insulating 15-UC LAO film using a Nb:STO substrate, but increasing the film thickness by 3 UC.<sup>22</sup> Namely, the dimensional crossover from three- to 2D electronic structures takes place between 7 and 6 UC in LNO/Nb:STO, but between 4 and 3 UC in LNO/LAO/Nb:STO. In Figs. 2(a) and 2(b), we presented only the ARPES spectra of the 10- and the 6-UC LNO films, because ARPES spectra before/after the dimensional crossover are qualitatively the same. After the dimensional crossover, the quasiparticle peaks in the  $e_g$  bands are significantly suppressed as seen vaguely in Fig. 2(b) (denoted by red dashed lines).

Finally, below 3 UC, we can observe a clear insulating band structure as shown in Fig. 2(c) for 2 UC. ARPES spectra for 3 UC are not presented, because they are nearly the same as for 2 UC except for peak-position shifts shown in Fig. 1. To see more clearly the band structure, we depicted the second derivative of ARPES spectra with respect to energy in Fig. 2(d). The topmost band with little dispersion originates from the  $t_{2g}$  bands and the dispersive band below

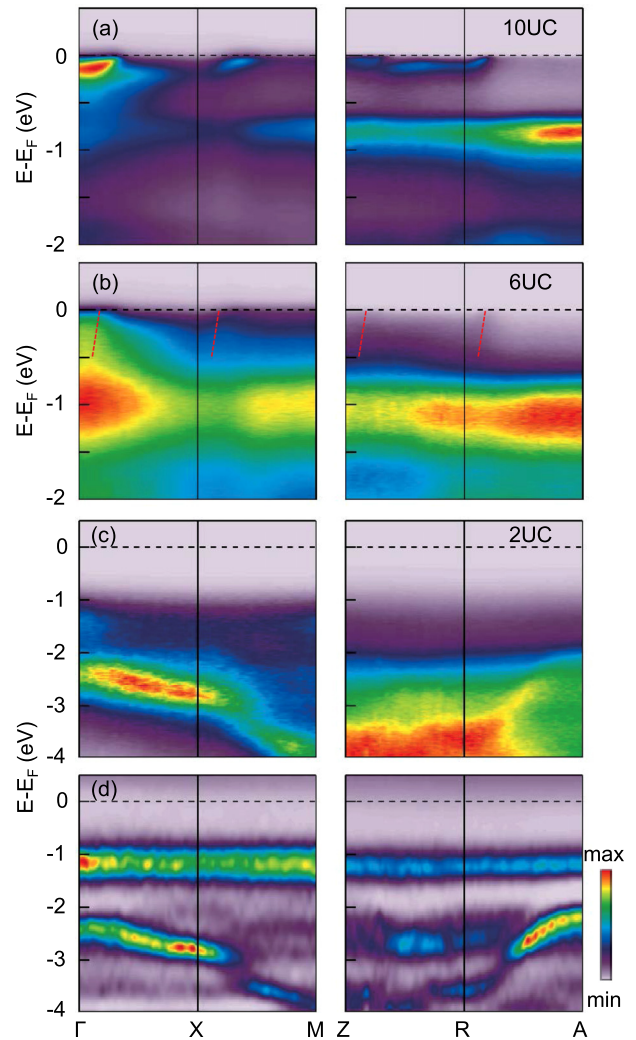


FIG. 2. Electronic band dispersions along the  $\Gamma XM$  and the  $ZRA$  lines for (a) 10-, (b) 6-, and (c) 2-UC LNO films on Nb:STO. (d) Second derivative of (c) with respect to energy. Vague quasiparticle bands are denoted by red dashed lines in (b).

$-2$  eV from the O  $2p$  bands, which guarantees good single crystallinity of our films down to 2 UC. We can see that the  $e_g$  bands are completely removed from the near- $E_F$  region to make an insulating gap. This insulating layer seems to play the same role as LAO in LNO/LAO/Nb:STO, because the ARPES spectra in LNO/Nb:STO above 4 UC change just like those in LNO/LAO/Nb:STO above 1 UC. Thus, we believe that a 3-UC insulating LNO film exists between metallic LNO and Nb:STO.

For the insulating-layer formation in the LNO/Nb:STO heterostructure, we can think of several possibilities: (1) Enhanced electron-electron correlations due to reduced dimensionality, (2) charge disproportionation as in other rare-earth nickelates,<sup>13,23</sup> and (3) nanometer-sized NiO precipitation.<sup>24</sup> The first possibility is easily ruled out, because as mentioned above, our previous study on LNO/LAO/Nb:STO shows that the reduced dimensionality is not enough to make a finite gap. Even when the film thickness is reduced down to 1 UC, the  $e_g$  bands still persist to form a Fermi surface and there is still a finite spectral weight at  $E_F$ .<sup>22</sup>

Second, if there is a rocksalt-type charge order as in other nickelates,<sup>13,23</sup> we can expect a band folding corresponding to

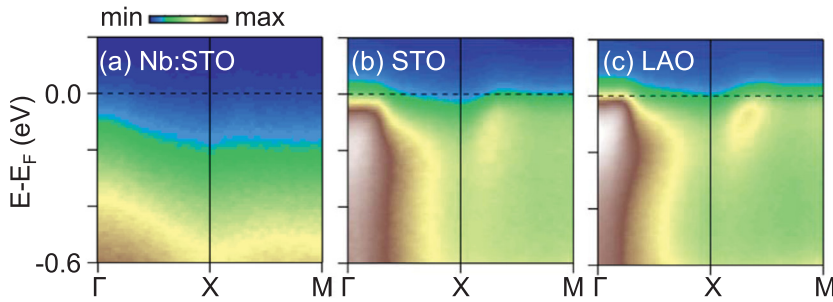


FIG. 3. (a)–(c) ARPES spectra along the  $\Gamma XM$  line of three 4-UC-thick LNO layers on Nb:STO, STO, and LAO/Nb:STO, respectively.

a charge-order wave vector  $\mathbf{q} = (1/2, 1/2, 1/2)$ . However, we could not find any hint of the band folding or Brillouin-zone reduction in the whole ARPES data. Under this situation, even if there is any charge order, the energy gap would be negligibly small.

Third, Detemple *et al.* reported that nanometer-sized NiO precipitates can be formed at the interface between polar LNO and nonpolar STO.<sup>24</sup> Since the NiO precipitates are Mott insulators, their presence at the interface can affect spectroscopic and transport properties. To resolve this issue, we compare the band structure of a 4-UC LNO film on STO with that on Nb:STO in Figs. 3(a) and 3(b), which shows they are totally different. Furthermore, the band structure of LNO/STO is quite similar to that of 4-UC LNO/LAO/Nb:STO shown in Fig. 3(c). This result strongly suggests that Nb doping in STO should be more crucial for the insulating-layer formation at the interface.

Then, let us consider the role of Nb doping at the LNO/Nb:STO interface. Since Nb:STO is a n-type semiconductor,<sup>9</sup> we can expect SB formation at the interface with metallic LNO as shown in Fig. 4(a). The work function  $W$  of LNO is about 4.5 eV (Ref. 25) and the electron affinity  $E_A$  of n-type semiconducting Nb:STO is about 3.9 eV,<sup>26</sup> thus the SB height is expected to be about 0.6 eV. Then, an electron transfer from Nb:STO to LNO takes place to make insulating LNO layers up to 3 UC as schematically shown in Fig. 4(b).

To confirm the SB formation, we measured the Sr 3d and Ti 2p core-level photoemission spectra of LNO/Nb:STO at  $h\nu = 200$  and 750 eV, respectively, which are presented in Fig. 5. We also depicted Sr 3d and Ti 2p core-level spectra of Nb:STO using bulk-sensitive Al  $K_{\alpha}$ . We can see gradual spectral changes that spectral weight at lower binding energy develops as the film thickness increases. The final peak shift is about 0.63 eV in Sr 2p, which is similar to the estimated SB height of LNO/Nb:STO and well-explained by the simple Schottky-Mott rule.<sup>26</sup> However, Ti 2p spectra shows a final

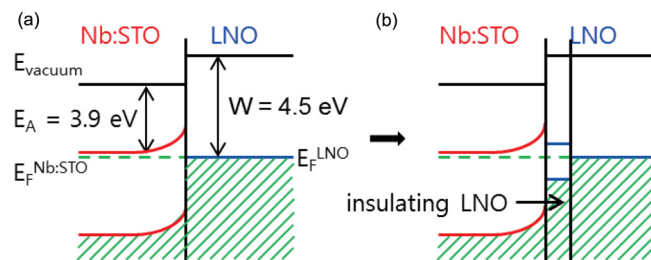


FIG. 4. Schematic diagrams of band alignment (a) for the SB formation and (b) for the formation of insulating LNO layers at the interface of LNO/Nb:STO.

shift of about 1.15 eV. This difference might be ascribed to the potential difference due to the polar layers of positive LaO and negative NiO<sub>2</sub> on top of the TiO<sub>2</sub> layer, which will reduce the binding energy of Ti 2p more than that of Sr 3d in addition to the shift by the SB formation.<sup>27</sup>

In the metallic LNO side, extra conduction electrons are doped within a screening length, called as “electrostatic doping.”<sup>28–30</sup> In conventional MS contact, the effect of the extra electron doping in the metallic region is negligible since the metal is considered as an electron reservoir. However, in a strongly correlated electron system, the electronic phases are very sensitive to the carrier doping even in a metallic phase.<sup>28,29</sup> Furthermore, a recent work<sup>30</sup> demonstrates that although the amount of the transferred electrons drops rapidly away from the interface, the modulation of the carrier concentration near the interface can be significant. For example, in a NdNiO<sub>3</sub> film on a La-doped STO substrate, the interfacial carrier concentration can be modulated larger than 20%.<sup>30</sup> Following this simple model, we estimated the

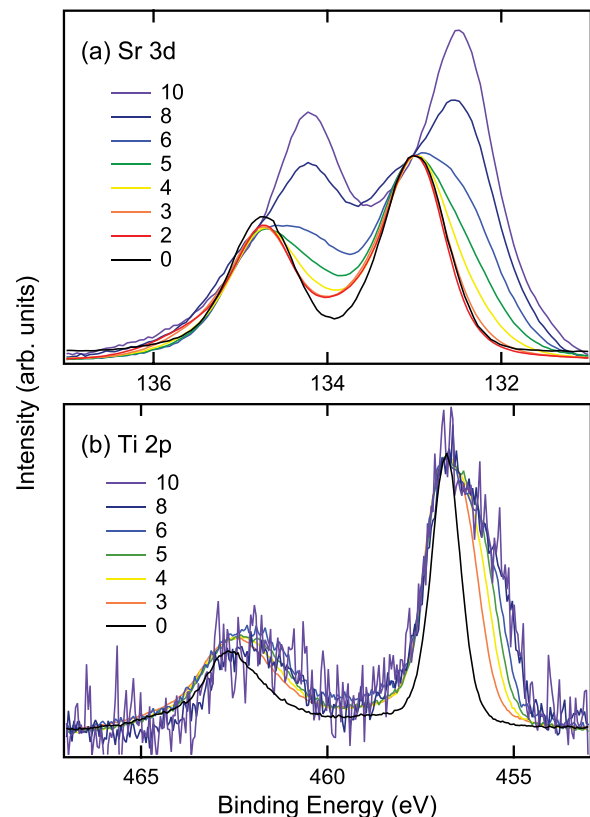


FIG. 5. (a) Sr 3d and (b) Ti 2p core-level photoemission spectra of LNO/Nb:STO heterostructures. Each spectrum was normalized at (a) 133 eV and (b) 456.75 eV.

modulation of the interfacial carrier concentration in our LNO film. The Thomas-Fermi screening length and the dielectric constant for LNO are about 0.6 nm and  $30\epsilon_0$ , respectively, which results in that the carrier modulation in a LNO film with 3 UC or less would be 5%–10%.

The ground-state electronic configuration of rare-earth nickelate is  $t_{2g}^6 e_g^1$ , and their metal-insulator transition (MIT) along the rare-earth series is ascribed to the variation of bandwidth or correlated covalency.<sup>31</sup> Usually, electron or hole doping drives a Mott insulator to become an exotic metal.<sup>32</sup> Thus, it is rather puzzling that a metallic LNO film with an integer-filling configuration can become an insulator by electron doping. Interestingly, metallic LNO becomes insulating as the oxygen-vacancy concentration increases.<sup>33</sup> Metallic SrFeO<sub>3</sub> also shows similar behavior when electrons are doped.<sup>34</sup> However, their energy gaps are much smaller than our results and have been attributed to enhanced charge disproportionation, which was discarded in the previous discussion on our insulating LNO layers. Thus, more elaborate studies are required.

Although the mechanism for the insulating-layer formation in LNO/Nb:STO is not clear at present, we suggest that it can provide an interesting functionality for a device, called as “Mottronics” that utilizes electronic-property changes between conducting and Mott insulating phases.<sup>35</sup> Our experiment demonstrates that the electronic phase of a ultrathin LNO film could be very sensitive to the carrier concentration. By designing a field effect transistor (FET) structure with an ultrathin LNO film as a conducting channel, we can achieve an electric-field-driven MIT. Additionally, we will be able to improve the device performance using ferroelectric materials as a gate insulator in the FET structure.<sup>28</sup> We also expect that an ultrathin LNO film would have a magnetic ordering accompanied with a MIT,<sup>14,16</sup> thus being applicable for spintronic devices.

In summary, we directly observed insulating-layer formation at the interface of LNO/Nb:STO by visualizing the electronic structure of ultrathin LNO films, combining *in situ* ARPES system with the state-of-the-art layer fabrication methods. We suggest that SB formation should be responsible for the insulating LNO layer at the interface.

The authors are grateful to S. I. Hyun, J. H. Shim, H. H. Nam, S. W. Han, S. B. Lee, and H. W. Park for helpful discussion. This work was supported by IBS-R009-D1. L.M. acknowledges support by a grant from the Swiss National Science Foundation (SNSF) (Project No. PBELP2-125484). Y.J.C. acknowledges support from National Research Foundation of Korea under Grant No. NRF-2014R1A1A1002868. The Advanced Light Source is supported by the Director, Office of Science, Office of Basic Energy Sciences, of the U.S. Department of Energy under Contract No. DE-AC02-05CH11231.

<sup>1</sup>H. Morkoç, S. Strite, G. B. Gao, M. E. Lin, B. Sverdlov, and M. Burns, *J. Appl. Phys.* **76**, 1363 (1994).

<sup>2</sup>H. C. Card and E. H. Rhoderick, *J. Phys. D: Appl. Phys.* **4**, 1589 (1971).

<sup>3</sup>R. K. Cavin, P. Lugli, and V. V. Zhirmov, *Proc. IEEE* **100**, 1720 (2012).

- <sup>4</sup>H. Y. Hwang, Y. Iwasa, M. Kawasaki, B. Keimer, N. Nagaosa, and Y. Tokura, *Nat. Mater.* **11**, 103 (2012).
- <sup>5</sup>J. H. Ngai, F. J. Walker, and C. H. Ahn, *Annu. Rev. Mater. Res.* **44**, 1 (2014).
- <sup>6</sup>M.-J. Lee, C. B. Lee, D. Lee, S. R. Lee, M. Chang, J. H. Hur, Y.-B. Kim, C.-J. Kim, D. H. Seo, S. Seo, U.-I. Chung, I.-K. Yoo, and K. Kim, *Nat. Mater.* **10**, 625 (2011).
- <sup>7</sup>S. Fusil, V. Garcia, A. Barthélémy, and M. Bibes, *Annu. Rev. Mater. Res.* **44**, 91 (2014).
- <sup>8</sup>K. van Benthem, C. Elsässer, and R. H. French, *J. Appl. Phys.* **90**, 6156 (2001).
- <sup>9</sup>K. Szot, W. Speier, G. Bihlmayer, and R. Waser, *Nat. Mater.* **5**, 312 (2006).
- <sup>10</sup>A. Ohtomo and H. Y. Hwang, *Nature* **427**, 423 (2004).
- <sup>11</sup>J. Garcia-Barriocanal, J. C. Cezar, F. Y. Bruno, P. Thakur, N. B. Brookes, C. Utfeld, A. Rivera-Calzada, S. R. Giblin, J. W. Taylor, J. A. Duffy, S. B. Dugdale, T. Nakamura, K. Kodama, C. Leon, S. Okamoto, and J. Santamaria, *Nat. Commun.* **82**, 1 (2010).
- <sup>12</sup>Y. Kozuka, M. Kim, C. Bell, B. G. Kim, Y. Hikita, and H. Y. Hwang, *Nature* **462**, 487 (2009).
- <sup>13</sup>J. B. Torrance, P. Lacorre, A. I. Nazzari, E. J. Ansaldo, and Ch. Niedermayer, *Phys. Rev. B* **45**, 8209 (1992).
- <sup>14</sup>A. V. Boris, Y. Matiks, E. Benckiser, A. Frano, P. Popovich, V. Hinkov, P. Wochner, M. Castro-Colin, E. Detemple, V. K. Malik, C. Bernhard, T. Prokscha, A. Suter, Z. Salman, E. Morenzoni, G. Cristiani, H.-U. Habermeier, and B. Keimer, *Science* **332**, 937 (2011).
- <sup>15</sup>J. Liu, S. Okamoto, M. van Veenendaal, M. Kareev, B. Gray, P. Ryan, J. W. Freeland, and J. Chakhalian, *Phys. Rev. B* **83**, 161102 (2011).
- <sup>16</sup>M. Gibert, P. Zubko, R. Scherwitzl, J. Íñiguez, and J.-M. Triscone, *Nat. Mater.* **11**, 195 (2012).
- <sup>17</sup>J. Chaloupka and G. Khaliullin, *Phys. Rev. Lett.* **100**, 016404 (2008).
- <sup>18</sup>P. Hansmann, X. Yang, A. Toschi, G. Khaliullin, O. K. Andersen, and K. Held, *Phys. Rev. Lett.* **103**, 016401 (2009).
- <sup>19</sup>Y. J. Chang, L. Moreschini, A. Bostwick, G. A. Gaines, Y. S. Kim, A. L. Walter, B. Freelon, A. Tebano, K. Horn, and E. Rotenberg, *Phys. Rev. Lett.* **111**, 126401 (2013).
- <sup>20</sup>K. Horiba, R. Eguchi, M. Taguchi, A. Chainani, A. Kikkawa, Y. Senba, H. Ohashi, and S. Shin, *Phys. Rev. B* **76**, 155104 (2007).
- <sup>21</sup>H. K. Yoo, S. I. Hyun, L. Moreschini, H.-D. Kim, Y. J. Chang, C. H. Sohn, D. W. Jeong, S. Sinn, Y. S. Kim, A. Bostwick, E. Rotenberg, J. H. Shim, and T. W. Noh, *Sci. Rep.* **5**, 8746 (2015).
- <sup>22</sup>H. K. Yoo, S. I. Hyun, Y. J. Chang, L. Moreschini, C. H. Sohn, H.-D. Kim, A. Bostwick, E. Rotenberg, J. H. Shim, and T. W. Noh, “Emergence of One Dimensionality by Thickness Control of Ultrathin in LaNiO<sub>3</sub> Films under Tensile Strain,” *Phys. Rev. X* (submitted).
- <sup>23</sup>V. Scagnoli, U. Staub, M. Janousch, A. M. Mulders, M. Shi, G. I. Meijer, S. Rosenkranz, S. B. Wilkins, L. Paolasini, J. Karpinski, S. M. Kazakov, and S. W. Lovesey, *Phys. Rev. B* **72**, 155111 (2005).
- <sup>24</sup>E. Detemple, Q. M. Ramasse, W. Sigle, G. Cristiani, H.-U. Habermeier, E. Benckiser, A. V. Boris, A. Frano, P. Wochner, M. Wu, B. Keimer, and P. A. van Aken, *Appl. Phys. Lett.* **99**, 211903 (2011).
- <sup>25</sup>T.-H. Yang, Y.-W. Harn, K.-C. Chiu, C.-L. Fan, and J.-M. Wu, *J. Mater. Chem.* **22**, 17071 (2012).
- <sup>26</sup>Y. Hikita, Y. Kozuka, T. Susaki, H. Takagi, and H. Y. Hwang, *Appl. Phys. Lett.* **90**, 143507 (2007).
- <sup>27</sup>M. Minohara, R. Yasuhara, H. Kumigashira, and M. Oshima, *Phys. Rev. B* **81**, 235322 (2010).
- <sup>28</sup>C. H. Ahn, J.-M. Triscone, and J. Mannhart, *Nature* **424**, 1015 (2003).
- <sup>29</sup>C. H. Ahn, A. Bhattacharya, M. D. Ventra, J. N. Eckstein, C. D. Frisbie, M. E. Gershenson, A. M. Goldman, I. H. Inoue, J. Mannhart, A. J. Millis, A. F. Morpurgo, D. Natelson, and J.-M. Triscone, *Rev. Mod. Phys.* **78**, 1185 (2006).
- <sup>30</sup>J. Son, B. Jalan, A. P. Kajdos, L. Balents, S. James Allen, and S. Stemmer, *Appl. Phys. Lett.* **99**, 192107 (2011).
- <sup>31</sup>S. R. Barman, A. Chainani, and D. D. Sarma, *Phys. Rev. B* **49**, 8475 (1994).
- <sup>32</sup>M. Imada, A. Fujimori, and Y. Tokura, *Rev. Mod. Phys.* **70**, 1039 (1998).
- <sup>33</sup>L. Qiao and X. Bi, *EPL* **93**, 57002 (2011).
- <sup>34</sup>Y. J. Xie, M. D. Scafetta, E. J. Moon, A. L. Krick, R. J. Sichel-Tissot, and S. J. May, *Appl. Phys. Lett.* **105**, 062110 (2014).
- <sup>35</sup>I. H. Inoue and M. J. Rozenberg, *Adv. Funct. Mater.* **18**, 2289 (2008).